Toward the equilibrium ground state of the charge density waves in rare-earth tritellurides

A. V. Frolov [1] A. P. Orlov,[1,2] A. Hadj-Azzem,[3] P. Lejay,[3] A. A. Sinchenko [1,4] and P. Monceau [3]

[1]*Kotelnikov Institute of Radioengineering and Electronics of RAS, 125009 Moscow, Russia*
[2]*Institute of Nanotechnologies of Microelectronics of RAS, 115487, Moscow, Russia*
[3]*Univ. Grenoble Alpes, CNRS, Grenoble INP, Institut Néel, 38000 Grenoble, France*
[4]*M.V. Lomonosov Moscow State University, 119991, Moscow, Russia*

We show that the charge density wave (CDW) ground state below the Peierls transition temperature T_{CDW} of rare-earth tritellurides is not at its equilibrium value, but depends on the time where the system was kept at a fixed temperature below T_{CDW}. This ergodicity breaking is revealed by the increase of the threshold electric field for CDW sliding which depends exponentially on time. We tentatively explain this behavior by the reorganization of the oligomeric $(Te_x)^{2-}$ sequence forming the CDW modulation.

I. INTRODUCTION

The collective motion (sliding) of charge density waves (CDWs) is one of the most fascinating properties of low-dimensional compounds exhibiting this type of electronic ordering. First predicted by Fröhlich [1] as dissipationless charge transfer, this type of electron transport is possible only when the electric field reaches a threshold electric field E_t. Impurities, defects, interchain interaction, or commensurability with the main lattice pin the phase of the CDW, and the conductivity in low electric fields $E < E_t$ demonstrates the conventional Ohmic behavior because of quasiparticle excitations. At $E > E_t$ the pinning is overcome and the CDW starts to slide, which is manifested as a sharp increase of conductivity. Such transport was previously observed and well studied in many inorganic and organic quasi-one-dimensional compounds [2,3].

Fröhlich considered the CDW as a macroscopic quantum state and suggested that there can be states with current flow if the CDW energy gap is displaced with the electrons and remains attached to the Fermi surface. This model was revised in Refs. [4–6]. If the electron dispersion is displaced by q, a Fröhlich collective current $j_{CDW} = nev$ is produced with $\hbar q = m^* v$, where m^* is the Fröhlich CDW mass. The Fröhlich model captures very well the CDW nonlinear transport properties [3]. In another electronic crystal, namely, $La_{1.875}Ba_{0.125}CuO_4$ with charge ordering (CO), a shift q in momentum of the CO peak was measured from femtosecond resonant x-ray scattering which can be interpreted as the CO condensate moving with momentum q following the Fröhlich model [7].

Recently, CDW sliding was also discovered in quasi-two-dimensional (quasi-2D) rare-earth tritellurides RTe_3 (R= La, Ce, Pr, Nd, Gd, Tb, Dy, Er, Tm) compounds [8,9]. The RTe_3 family has an orthorhombic crystal structure (space group C_{mcm}) and consists of double Te planes separated by corrugated RTe planes. In this space group, the b axis is perpendicular to Te planes. All these compounds exhibit a transition to a state with an incommensurate unidirectional charge density wave with a wave vector $\mathbf{Q}_{CDW1} = (0, 0; \sim \frac{2}{7}c^*)$ at the Peierls temperature higher than 250 K. For heavy R elements (Dy, Ho, Er, Tm), a second transition to a state with an independent charge density wave with the wave vector $\mathbf{Q}_{CDW2} = (\sim \frac{2}{7}a^*, 0, 0)$ perpendicular to $\mathbf{Q}_{CDW1}$ occurs at low temperatures. The sharpness of superstructure maxima in x-ray diffraction indicates the existence of a three-dimensional long-range order [10].

In this paper, we report a new effect in the nonlinear CDW dynamics observed in $TbTe_3$. The threshold electric field increases dramatically under isothermal exposition of the sample at a fixed T_{expt} below T_{CDW} during several hours. The temperature dependence of E_t after such a procedure demonstrates a strong peak effect with a maximum at T_{expt}. Some similarity can be found with the peak effect in superconductors [11]. These effects have never been observed in quasi one-dimensional (1D) CDW systems.

II. EXPERIMENTAL

Figure 1(a) shows a sketch of the crystal structure of $TbTe_3$. The lattice parameters of $TbTe_3$ are $a = 4.29$ Å, $b = 25.33$ Å and $c = 4.303$ Å. A CDW with a Peierls transition at $T_{CDW} = 336$ K develops along the c axis with the wave vector $\mathbf{Q}_{CDW1} = (0, 0, 0.296)$. A CDW has also been reported [12] below $T \sim 41$ K along the a axis with a wave vector $\mathbf{Q}_{CDW2} = (0.32, 0, 0)$. Although the in-plane lattice parameters are almost identical, the Te planes are essentially square with the C_4 symmetry. As shown by Yao *et al.* in Ref. [13], a CDW in a layered quasi-2D system with a tetragonal symmetry can be either bidirectional (checkerboard) or unidirectional. They derived a phase diagram as a function of the electron-phonon coupling. With a strong electron coupling the CDW is unidirectional, as is the case in RTe_3 compounds for which the structure is fundamentally orthorhombic because of the glide
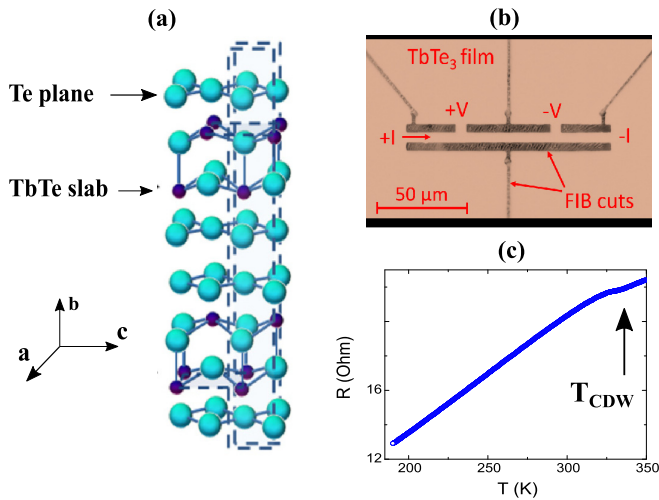
FIG. 1. (a) Sketch of the TbTe$_3$ structure. (b) Optical microscope image of the typical bar structure based on a TbTe$_3$ single crystal. (c) Typical temperature dependence of resistance, $R(T)$, for one of the structures.

plane between the adjacent Te layers [14]. Single crystals of this compound were grown in a pure argon atmosphere by the technique described in our previous work [8]. Thin rectangular single-crystal samples thinner than 1 μm were prepared by the micromechanical exfoliation of relatively thick crystals preliminarily glued to a sapphire substrate. The quality of crystals and the spatial position of the crystallographic axes were monitored by x-ray diffraction. Bar structures oriented along c axis with a length of 70–150 μm and a width of 5–10 μm were prepared by etching with the use of a focused ion beam [Fig. 1(b)]. One such structure is shown in Fig. 1(b). Resistances, current-voltage characteristics (*IV*Cs) and their derivatives dV/dI, of these structures were measured by the four-probe method. Typical temperature dependence of resistance for one of a structure is shown in Fig. 1(c). It can be seen that the resistivity peculiarity corresponding to the CDW transition at $T = 336$ K is very weak, which is typical for resistivity along the c-axis direction, which is in accordance with the results of Ref. [15]. The time evolution of the *IV*Cs at a stabilized temperature was measured automatically with a fixed time interval, typically 30–60 minutes, during several tens of hours.

III. EXPERIMENTAL RESULTS

In usual experimental condition when the TbTe$_3$ sample is cooled from $T > T_{CDW}$ at the rate 3–5 K/min, the temperature dependence of the threshold electric field $E_t(T)$ is of the order of 10^2 mV/cm and reproduces the behavior previously reported in Ref. [9], that is to say, a nearly linear increase when T is decreased. However, we noticed that E_t increases significantly if the sample is kept at a fixed T_{expt} below T_{CDW1} a sufficiently long time [16]. To study this effect the experimental procedure was the following: we cooled the sample from $T > T_{CDW1}$ down to a given temperature T_{expt} and measured *IV*Cs with a time interval of 30 minutes during several tens of hours and that at different T_{expt} in the range 220–330 K. Before each exposition the sample was warmed above T_{CDW1}.
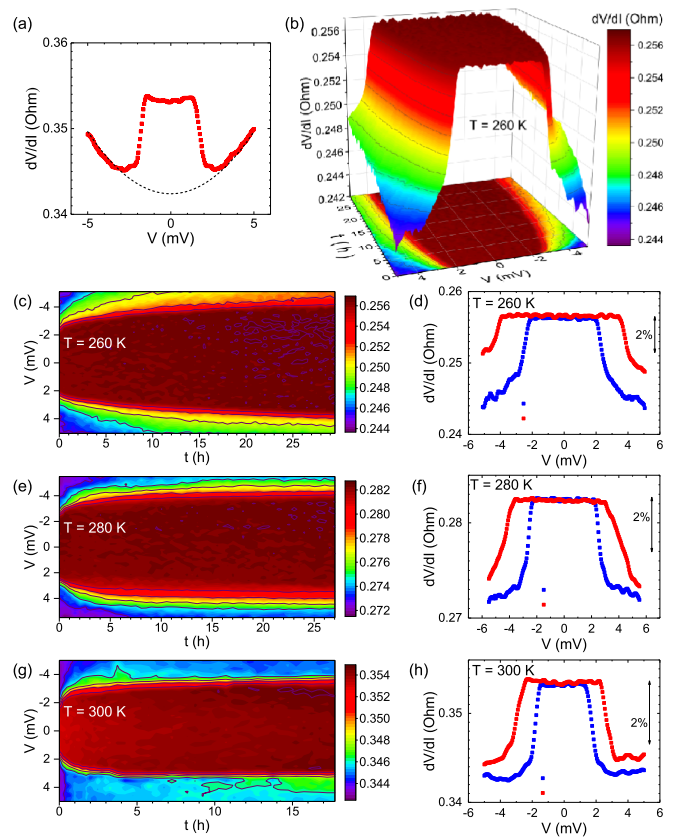

FIG. 2. (a) Original differential current-voltage characteristic, $dV/dI(V)$, at $T = 260$ K. Dashed line shows the parabolic background corresponding to Joule heating. (b) Three-dimensional plot of time evolution of differential IVs after subtraction of Joule heating. (c), (e), (g) Evolution of differential *IV*Cs with time for $T_{expt} = 260$, 280, and 300 K. (d), (f), (h) Initial (blue) and final (red) differential IVs with substraction of Joule heating for the same temperatures.

For more clarity we extracted the parabolic contribution of Joule heating [dashed line in Fig. 2(a)] from the original IVs. A three-dimensional plot illustrating measurements is shown in Fig. 2(b) for $T_{expt} = 260$ K. In Figs. 2(c), 2(e), and 2(g) we show the evolution of differential *IV*Cs with time for one of the samples for $T_{expt} = 260$, 280, and 300 K, respectively. Figures 2(d), 2(f), and 2(h) represent the initial and final $dV/dI(V)$ for the corresponding T_{expt}. It can be seen that the threshold electric field really increases with time and saturates at a certain value of t. This characteristic time depends on the chosen T_{expt}. This time evolution of the threshold is more pronounced for higher values of T_{expt} for which E_t increases more than two times.

It is seen in Figs. 2(d), 2(f) and 2(h) that, in addition in the change in the value of E_t, the drop of resistance at the threshold, which determines the contribution of the sliding of the CDW to electron transport, is significantly less at low T_{expt}. The contribution of the collective motion of the CDW to the total transport current is determined by the number of carriers condensed in the CDW state and the velocity of the CDW. In our case, the number of carriers condensed below the CDW gap should be the same and not depend on the thermal treatment at T_{expt}. Consequently, the sliding velocity of the CDW determined by friction effects for exposed samples is
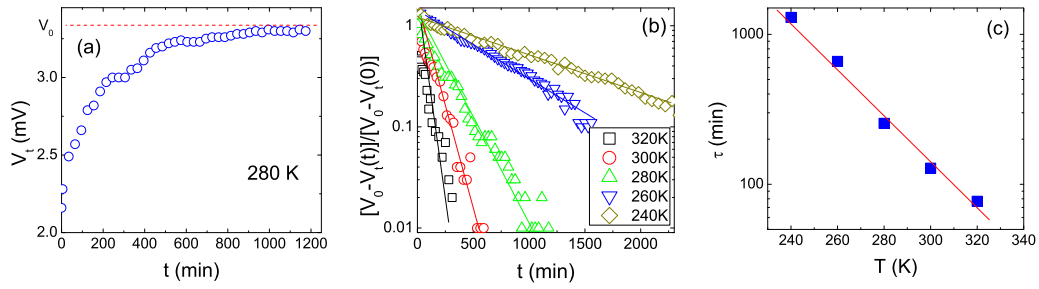
FIG. 3. (a) Dependence $V_t(t)$, where V_t is the threshold voltage, at $T_{expt} = 280$ K. (b) semilogarithmic plot of $[V_0 - V_t(t)]/[V_0 - V_t(t = 0)]$ for $T_{expt} = 320$ K (black squares), 300 K (red circles), 280 K (green triangles), 260 K (blue inverted triangles), and 240 K (gray rhombuses). (c) Temperature dependence of relaxation time τ deduced from panel (b) as a function of temperature in a semilogarithmic plot.

much lower. Note that the resistance at $V = 0$ remains the same [16] independent of the exposition time at all T_{expt} as seen in Figs. 2(d), 2(f), and 2(h). The resistance in the CDW static state is determined by carrier scattering on the Fermi surface reduced by the opening of the CDW energy gap which does not change with time at any T_{expt}. Thus, this result is the direct indication that all the changes in the sample during the exposition take place in the CDW subsystem.

Figure 3(a) shows the dependence of $V_t(t)$, where V_t is the threshold voltage, at $T_{expt} = 280$ K. As can be seen, the threshold voltage, $V_t(t)$ rapidly increases at short time and saturates at a value V_0 at larger time. To determine the characteristic time of the $V_t(t)$ evolution, we plot in Fig. 3(b) the dependencies of $[V_0 - V_t(t)]/[V_0 - V_t(t = 0)]$ for different T_{expt} on a logarithmic scale. At all temperatures $V_0 - V_t(t) \sim 1 - \exp(t/\tau)$ with the characteristic time τ strongly temperature dependent. As can be seen from Fig. 3(c), τ depends exponentially on temperature as $\tau \sim \exp(-\frac{T}{T_0})$, with $T_0 \approx 30$ K.

Let us consider the temperature dependence of the threshold electric field. As reported in Ref. [9], when the temperature continuously decreased from T well above $T_{CDW1} = 336$ K, the temperature of the threshold electric field demonstrates a nearly linear increase. For samples not exposed at T_{expt} for a given time, the dependence $E_t(T)$ is completely reversible. Another picture is observed for samples exposed a long time at a fixed T_{expt}. These samples were cooled from $T > T_{CDW1}$ down to T_{expt}, kept at this temperature for a given time and then cooled down to $T = 190$ K with a rate 5 K/min, then IV curves were measured under warming with a fixed temperature step ΔT. For each step, the temperature was regulated with an accuracy of 0.1 K. Figure 4(a) shows a set of IV Cs in the temperature range 190–330 K for a sample which was exposed during 20 hours at $T = 300$ K. Fig. 4(b) shows IV curves for the same sample but without exposition, the measurements have been performed similarly as in Ref. [9]. It is seen that the characteristics in Fig. 4(b) are in agreement with known results [9]: the threshold field increases monotonically when T is decreased, demonstrating a nearly linear dependence. The picture changes qualitatively when the sample is exposed at 300 K. The threshold field increases significantly in the entire temperature interval, excluding a narrow range near T_{CDW}. The dependence $E_t(T)$ becomes nonmonotonic with a maximum near $T = T_{expt}$ [Fig. 4(a)].

Qualitatively the same picture is observed for different T_{expt}. As an example, Figs. 4(c) and 4(d) demonstrate corresponding temperature evolutions of differential IVs: under warming from 190 K up to 330 K for a sample which was exposed during 20 hours at $T_{expt} = 260$ K [Fig. 4(c)] and under continuous cooling the same sample from 330 K up to 190 K [Fig. 4(d)]. The curves in Fig. 4(d) show a nearly linear
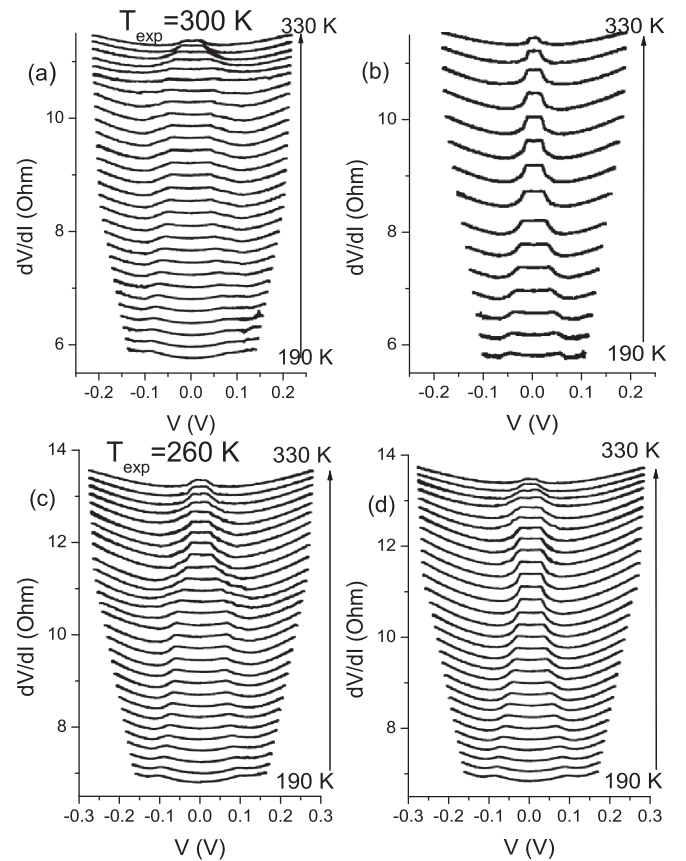

FIG. 4. (a) Differential IVs measured under continuous warming in a temperature range 190–330 K with a step $\Delta T = 5$ K of TbTe$_3$ exposed at $T_{expt} = 300$ K during 20 hours. (b) Differential current-voltage characteristics measured over the same temperature range with a step $\Delta T = 10$ K for the same sample during continuous cooling from $T = 350$ K. (c) The same as in panel (a) but for $T_{expt} = 260$ K. (d) Differential IV Cs during continuous cooling from $T = 330$ K after warming in panel (c).
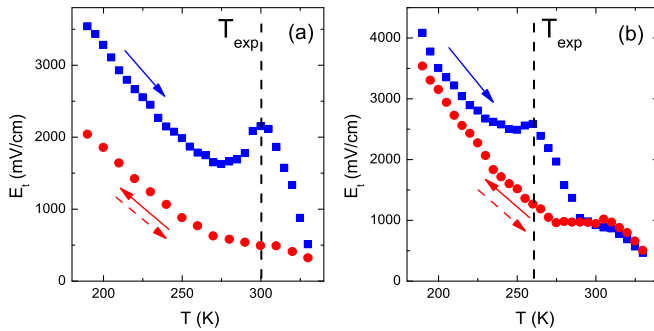
FIG. 5. Temperature dependence of the threshold electric field E_t for the CDW sliding for exposed samples (blue squares) and nonexposed (red circles) for (a) $T_{expt} = 300$ K and (b) 260 K. Red dots correspond to E_t when the sample is continuously cooled at a rate of a few degrees per minute from $T > T_{CDW1}$ down to 190 K. Blue squares are values of E_t measured during warming when the sample was exposed at (a) $T_{expt} = 300$ K and (b) 260 K for a long time and then cooled to 190 K. The maximum of E_t occurs at the temperature of exposition, T_{expt}, as shown by the dashed lines in panels (a) and (b).

increase of E_t when T decreases while the curves in Fig. 4(c) show a strong maximum near $T = T_{expt} = 260$ K.

One question that has to be considered is that the effect on the value of E_t depends on the time that the sample is in the nonlinear state. Let us recall the experimental procedure: at T_{expt}, IVCs are measured every half hour and the time for recording each IVC is approximately 1 minute. Thus, the time at which the voltage is above the threshold is two orders of magnitude with respect to that in the static state. We then conclude that the time spent at T_{expt} determines the evolution of E_t. Temperature dependencies of $E_t(T)$ for both cases shown in Fig. 4 for $T_{expt} = 300$ K [Fig. 4(a)] and 260 K [Fig. 4(b)] are drawn in Fig. 5. Red circles correspond to E_t values measured when T is continuously decreased from $T > T_{CDW1}$ for Fig. 5(a) or continuously decreased from $T = 330$ K for Fig. 5(b). Blue squares correspond to E_t values when, the temperature being reduced from $T > T_{CDW1}$ and kept fixed at $T = T_{expt} < T_{CDW}$ for enough time to reach saturation as shown in Fig. 3, T is continuously increased from $T = 190$ K, manifesting sharp maxima at $T \sim T_{expt}$. Note that the $E_t(T)$ dependencies without or with exposition at $T = 260$ K become identical 30–40 K above $T = T_{expt}$, as seen in Fig. 5(b).

IV. DISCUSSION

We thus report the time effect on the value of the threshold field E_t for CDW compounds exhibiting sliding. Corresponding as mentioned above that the Ohmic resistivity of the samples remains unchanged during exposition [see Figs. 2(d), 2(f), and 2(h)], it means that there are no lattice defects created during the exposition times which may act as new pinning centers. Thus, the strong increase of E_t with time should result from some modification of pinning conditions: the appearance of a stronger pinning when the CDW tends to equilibrium ground state.

Let us recall that two types of pinning are usually distinguished: collective or weak pinning, where, from an internal random summation of the pinning forces from over a great number of impurities in a domain, the CDW phase deviation to ideality is on the order of π, and the local or strong pinning where the CDW phase is located at each impurity and produces local metastable states– - plastic deformation or dislocation loops—with finite barriers. Competition between weak and strong pinning was perfectly illustrated in the explanation of the low-frequency peak in the real part of the dielectric response [17]. With the decrease of temperature because of the reduction of screening and exponentially vanishing of the number of free carriers, the weak pinning is exhausted; the pinning becomes essentially locally induced by strong pinning impurities which only are effective for initiating plastic deformations and metastable states in the CDW superstructure, thus dominating the kinetic properties of the system. These low-energy excitations (LEEs) contribute also at temperatures below 1 K in thermodynamical properties as an additional contribution to the specific heat of the regular phonon term. These LEEs were interpreted as metastable states and analyzed as two-level systems resulting from local deformation of the CDW at strong pinning impurity centers [18]. In this low-T range the relaxation of these metastable states has the form of a stretched exponential reflecting the wide time distribution. The breakdown of the collective pinning and the crossover to strong pinning of vortices has also been proposed for the explanation of the "peak effect," namely, the maximum of the critical current as a function of magnetic field or temperature observed in low- and high-temperature superconductors [19,20].

Collective electron transport in RTe$_3$ compounds is possible only along the direction of the CDW wave vector [9]. Although having all signatures of the sliding of a charge density wave, there are significant differences with the CDW sliding in quasi-1D systems: (i) the coherent x-ray diffraction pattern in TbTe$_3$ remains nearly identical to the same distribution of speckles up to the threshold, unlike the 1D NbSe$_3$ in which the CDW is strongly deformed below E_t; (ii) at E_t the CDW is suddenly depinned and the $2k_F$ wave vector Q_{CDW1} slightly rotates with an atypical angle of $0.002°$, while no compression or dilatation is observed for the component of Q_{CDW1} along the c axis. There is a CDW shear manifested by a small component of Q_{CDW1} along the a and b axes transverse to the CDW wave vector [21,22]; (iii) an anomalously small temperature-independent contribution of the CDW motion to the total electron transport determined by the ratio $\Delta R/R$ (ΔR is the relative change in the resistance at sliding and R is the total resistance), which indicates a very low velocity of this motion in a given electric field; (iv) a linear dependence of $E_t(T)$ [9]. Note that the threshold field in quasi-1D compounds increases exponentially below T_{CDW} [23]. These results indicate a fundamental difference in sliding mechanisms and, therefore, in pinning mechanisms in 1D and 2D compounds.

Tellurium, being the least electronegative element among chalcogens, can stabilize longer than normal bond distances which associate through Te-Te bonding interaction: from the superspace crystallographic technique, it was shown that the CDW modulation in RTe$_3$ compounds can be defined as a

sequence in the Te planes of oligomeric fragments of $(Te_x)^{2-}$, typically trimers or tetramers, and even single Te atoms. For instance, the detailed temperature dependence of the incommensurate CDW modulation of $SmTe_3$ can be described as such a sequence of trimers and tetramers. As the temperature is increased, the distribution of Te-Te bonds changes and the connectivity of the oligomers now results in a different sequence of trimers and tetramers [24,25].

Then one can interpret the time dependence of the threshold field as follows: cooling $TbTe_3$ from $T > T_{CDW1}$ at a uniform rate the sequence of oligomers which defines the CDW modulation is metastable with many defects. Keeping the temperature fixed at T_{expt}, the oligomeric sequence reorganizes and reaches after a certain time (longer at low temperature) the equilibrium state. A possible mechanism is hopping of Te between trimer and tetramer fragments or the participation of single Te atom in bonding. At equilibrium the CDW superstructure is more ordered with domains whose walls can pin the CDW phase collectively, then increasing the threshold field. We assume that, under the increase of T above T_{expt}, the sequence of oligomers becomes metastable again demonstrates some kind of melting. As a result, the crossover from weak collective pinning to strong individual pinning takes place, leading to a strong increase of E_t and the appearance of a sharp maximum in the $E_t(T)$ dependence. In the frame of this scenario the processes of ordering and disordering of the oligomer sequence are operated by the thermal fluctuations.

This effect of reorganization of the CDW with time should be observable in high-resolution x-ray diffraction since only small change either in the modulation wave vector and/or of the width of the satellite peak are expected. Our x-ray experiment in Ref. [21] was performed at room temperature where the CDW satellite was detected after a time largely more where the equilibrium state was reached. The experiment to be performed when it will be possible, with the ESRF beam line perfectly aligned on the CDW satellite in a sample kept a long enough time at fixed $T^* < T_{CDW1}$, to warm the sample above $T_{CDW1} = 336$ K and cool it down again to T^* and remeasure immediately the satellite profile to see if there are any changes, such a possible time and/or temperature dependence of the rotation of the Q vector, hoping that the temperature excursion will not misalign the beam line.

In conclusion, we have shown that, when cooled at the rate of a few degrees/min through the Peierls phase transition, the CDW ground state of the rare-earth tritelluride $TbTe_3$ is not at the equilibrium, but time dependent. This is reflected by the increase of the threshold electric field for depinning the CDW and initiation of the sliding with an exponential dependence on time. This phenomenon was not observed for quasi-one-dimensional CDWs and appears to be specific to the two-dimensional nature of the RTe_3 compound, specifically linked to Te-Te bonding with different bond distances that form the charge modulation. More experiments to fully describe the phenomenon, namely, by quenching the sample through T_{CDW1} or by cooling it through T_{CDW1} down to T^* under an electric field larger the threshold field at T^*, are underway.

[1] H. Fröhlich, Proc. R. Soc. A **223**, 296 (1954).

[2] G. Gruner, *Density Waves in Solids* (Addison-Wesley, Reading, 1994).

[3] P. Monceau, Adv. Phys. **61**, 325 (2012).

[4] D. Allender, J. W. Bray, and J. Bardeen, Phys. Rev. B **9**, 119 (1974).

[5] J. Bardeen, Phys. Rev. Lett. **55**, 1010 (1985).

[6] J. Bardeen, Phys. Rev. B **39**, 3528 (1989).

[7] M. Mitrano, S. Lee, A. A. Husain, M. Zhu, G. de la Peña Munoz, Stella X.-L. Sun, Young Il Joe, Alexander H. Reid, Scott F. Wandel, Giacomo Coslovich *et al.*, Phys. Rev. B **100**, 205125 (2019).

[8] A. A. Sinchenko, P. Lejay, and P. Monceau, Phys. Rev. B **85**, 241104(R) (2012).

[9] A. A. Sinchenko, P. Lejay, O. Leynaud, and P. Monceau, Solid State Commun. **188**, 67 (2014).

[10] N. Ru, C. L. Condron, G. Y. Margulis, K. Y. Shin, J. Laverock, S. B. Dugdale, M. F. Toney, and I. R. Fisher, Phys. Rev. B **77**, 035114 (2008).

[11] A. I. Larkin and Yu. N. Ovchinnikov, J. Low Temp. Phys. **34**, 409 (1979).

[12] A. Banerjee, Y. Feng, D. M. Silevitch, J. Wang, J. C. Lang, H.-H. Kuo, I. R. Fisher, and T. F. Rosenbaum, Phys. Rev. B **87**, 155131 (2013).

[13] H. Yao, John A. Robertson, E.-A. Kim, and S. A. Kivelson, Phys. Rev. B **74**, 245126 (2006).

[14] H.-M. Eiter, Michela Lavagnini, Rudi Hackl, Elizabeth A. Nowadnick, Alexander F. Kemper, Thomas P. Devereaux, J.-H. Chu, James G. Analytis, Ian R. Fisher, and L. Degiorgi, Proc. Natl. Acad. Sci. USA **110**, 64 (2013).

[15] A. A. Sinchenko, P. D. Grigoriev, P. Lejay, and P. Monceau, Phys. Rev. Lett. **112**, 036601 (2014).

[16] F. V. Frolov, A. P. Orlov, A. A. Sinchenko, and P. Monceau, JETP Lett. **109**, 203 (2019).

[17] A. Larkin and S. Brasovskii, Solid State Commun. **93**, 275 (1995).

[18] K. Biljakovic, J. C. Lasjaunias, P. Monceau, and F. Levy, Phys. Rev. Lett. **62**, 1512 (1989).

[19] A. C. Marley, M. J. Higgins, and S. Bhattacharya, Phys. Rev. Lett. **74**, 3029 (1995).

[20] W. K. Kwok, J. A. Fendrich, C. J. van der Beek, and G. W. Crabtree, Phys. Rev. Lett. **73**, 2614 (1994).

[21] D. Le Bolloc'h, A. A. Sinchenko, V. L. R. Jacques, L. Ortega, J. E. Lorenzo, G. A. Chahine, P. Lejay, and P. Monceau, Phys. Rev. B **93**, 165124 (2016).

[22] E. Bellec, Ph.D. thesis, Université Paris-Saclay, 2019.

[23] K. Maki, Phys. Rev. B **33**, 2852 (1986).

[24] D. Malliakas and M. G. Kanatzidis, J. Am. Chem. Soc. **128**, 12612 (2006).

[25] H. J. Kim, C. D. Malliakas, A. T. Tomić, S. H. Tessmer, M. G. Kanatzidis, and S. J. L. Billinge, Phys. Rev. Lett. **96**, 226401 (2006).